Key Points:
- Antarctic ice core data provide supporting evidence for the bipolar seesaw mechanism during the early last interglacial period
- Model experiments of the bipolar seesaw mechanism during the last interglacial partially reconcile the Antarctic ice core anomaly
- We simulate 50–60% of the peak Southern Ocean sea surface temperature anomaly, winter sea ice retreat, and ice core isotope enrichment

Simulating the 128-ka Antarctic Climate Response to Northern Hemisphere Ice Sheet Melting Using the Isotope-Enabled HadCM3

Max D. Holloway[1,2,3] [ID], Louise C. Sime[2] [ID], Joy S. Singarayer[4] [ID], Julia C. Tindall[5] [ID], and Paul J. Valdes[3] [ID]

[1]Data Science Division, National Physical Laboratory, Teddington, UK, [2]Ice Dynamics and Paleoclimate, British Antarctic Survey, Cambridge, UK, [3]School of Geographical Sciences, University of Bristol, Bristol, UK, [4]Department of Meteorology, University of Reading, Reading, UK, [5]School of Earth and Environment, University of Leeds, Leeds, UK

Abstract Warmer than present Antarctic and Southern Ocean temperatures during the last interglacial, approximately 128,000 years ago, have been attributed to changes in north-south ocean heat transport, causing opposing hemispheric temperature anomalies. We investigate the magnitude of Antarctic warming and Antarctic ice core isotopic enrichment in response to Northern Hemisphere meltwater input during the early last interglacial. A 1,600-year HadCM3 simulation driven by 0.25 Sv of meltwater input reproduces 50–60% of the peak Southern Ocean summer sea surface temperature anomaly, sea ice retreat, and ice core isotope enrichment. We also find a robust increase in the proportion of cold season precipitation during the last interglacial, leading to lower isotopic values at the Antarctic ice core sites. These results suggest that a HadCM3 simulation including 0.25 Sv for 3,000–4,000 years would reconcile the last interglacial observations, providing a potential solution for the last interglacial *missing heat* problem.

Plain Language Summary The Antarctic isotope and temperature maximum, which occurred approximately 128,000 years Before Present (yBP) during the warmer than present last interglacial period, is hypothesized to have resulted from a slowdown in northward ocean heat transport due to ice sheet melting into the North Atlantic—a mechanism known as the bipolar seesaw. We test this hypothesis by running and analyzing long, fully coupled, isotope-enabled climate model simulations, which include meltwater entering the North Atlantic, for this critical period 128,000 yBP. Results are evaluated against ocean and ice core data. After 1,600 years, we simulate 55% of the peak Southern Ocean summer sea surface temperature anomaly, 50% of the estimated winter sea ice retreat, and 60% of the ice core isotope enrichment reconstructed during the early last interglacial Antarctic climate optimum.

1. Introduction

During past deglaciations, large volumes of glacial meltwater entered the North Atlantic Ocean from Northern Hemisphere ice sheets (Bond & Lotti, 1995; Broecker & Henderson, 1998; Clark et al., 2002; Duplessy et al., 1992; Peltier, 2004). The input of meltwater to the North Atlantic tends to decrease surface density and weaken the Atlantic Meridional Overturning Circulation (AMOC), and the associated cross-equatorial ocean heat transport (Peltier & Vettoretti, 2014; WAIS Divide Project Members, 2013, 2015). Hence, this is one mechanism that could drive a bipolar seesaw mechanism, where the south (north) warms while the north (south) tends to cool (Stocker & Johnsen, 2003).

During the penultimate deglaciation, large magnitudes of glacial meltwater entered the North Atlantic Ocean during Heinrich Stadial 11 (HS11; Broecker & Henderson, 1998; Govin et al., 2012; Marino et al., 2015). HS11 peaked at 0.3 ± 0.04 Sv (1 Sv = 10^6 m^3/s) around 133 thousand years ago (ka) and decreased to ~0.05 Sv by 128 ka (Marino et al., 2015). It appears that HS11 led to delayed warming in the Northern Hemisphere and preceded an early last interglacial (LIG; 130 to 115 ka) climate optimum in the Southern Hemisphere (Govin et al., 2015; Marino et al., 2015), most clearly evident as a maximum in Antarctic ice core stable water isotope ($\delta^{18}O$ and δD) records at approximately 128 ka (Masson-Delmotte et al., 2011; Sime et al., 2009). By applying a modern $\delta^{18}O$-temperature calibration, these records have been used to infer Antarctic air temperatures that were >4 °C above present (Jouzel et al., 2007; Sime et al., 2009). Additionally, marine sediment core evidence

suggests that Southern Ocean summer sea surface temperatures (SSST) were ~2 °C warmer than present at 128 ka (Capron et al., 2014; 2017; Hoffman et al., 2017).

It has been postulated that half of the Antarctic warming that occurred by the end of HS11 can be accounted for by changes in radiative forcing, leaving an excess *residual* warming that has been attributed to heat accumulation in the Southern Hemisphere in response to a suppressed AMOC (Govin et al., 2012; Marino et al., 2015). Previous work has tested this hypothesis using relatively short, 200-year-long atmosphere-ocean coupled climate model experiments including meltwater input to the North Atlantic Ocean during the early LIG but conclude that this mechanism alone is insufficient to reconcile inferred Antarctic temperatures (e.g., Holden et al., 2010; Stone et al., 2016). We revisit this question utilizing 1,600-year-long isotope-enabled coupled climate model simulations with meltwater input to the North Atlantic Ocean. These experiments enable quantification of the role of meltwater from retreating Northern Hemisphere ice sheets on Antarctic climate and the ice core isotope record during the early LIG.

## 2. Methods

2.1. Climate Model Experiments

We carry out a series of isotope-enabled (Holloway, Sime, Singarayer, Tindall, & Valdes, 2016; Tindall et al., 2009) coupled atmosphere-ocean general circulation model experiments using the U.K. MetOffice HadCM3 model. The simulated distribution of isotopes in Antarctic precipitation compare well to present-day observations (e.g., Sime et al., 2008). Our series of simulations focusses on the LIG Antarctic isotope maximum, centered at 128 ka, and include different magnitudes of meltwater entering the North Atlantic. We perform four primary experiments, each with orbital, greenhouse gas concentrations and ice sheet configuration fixed at 128-ka values and with (i) no meltwater forcing and (ii) 0.1, (iii) 0.2, and (iv) 0.25 Sv of meltwater added to the surface North Atlantic Ocean. Note, the 0.2 and 0.25 cases both exceed the limit for AMOC collapse in HadCM3 (Stone et al., 2016).

Meltwater is added uniformly to the surface North Atlantic Ocean between 45° and 70°N. The actual meltwater isotopic composition from deglaciating Northern Hemisphere Ice Sheets is highly uncertain (e.g., Ferguson & Jasechko, 2015; Hill et al., 2006). We set the ocean isotopic composition to 0‰ (equivalent to present day) to ensure no negative drift in whole ocean isotopic composition. We therefore use the assumption that by the end of HS11 or coincident with the 128-ka isotope data, sea level has reached approximately present-day values, resulting in a globally integrated ocean isotopic composition of 0‰.

All climatologies were calculated using the final 30 years of each experiment and are compared to a preindustrial control simulation (PI). The PI experiment has been time integrated for 800 years to reach a pseudo-equilibrium state (i.e., drifts in the atmosphere, surface, and middepth ocean become negligible). The 128-ka experiment with no meltwater forcing (NOFW) was integrated for 700 years to reach the same pseudo-equilibrium state. Each of the meltwater forcing experiments were continued from NOFW with the inclusion of North Atlantic meltwater forcing. The 0.1-Sv case was continued for an additional 400 years, the 0.2 Sv for 1,000 years, and the 0.25-Sv case for 1,600 years. These experiments represent significantly longer meltwater forcing scenarios than previous LIG experiments run with the HadCM3 model (Holden et al., 2010; Stone et al., 2016). We present the climate response for all meltwater experiments (0.1, 0.2, and 0.25 Sv) but concentrate our analysis of the isotope response on the highest meltwater scenario of 0.25 Sv.

2.2. Ice and Ocean Core Data

We compare model isotope output against five published ice core records from East Antarctica (Masson-Delmotte et al., 2011): Vostok (Petit et al., 1999), Dome F (DF; Kawamura et al., 2007), European Project for Ice Coring in Antarctica (EPICA) Dome C (EDC; Jouzel et al., 2007), EPICA Dronning Maud Land (EDML; EPICA Community Members, 2006), and Talos Dome Ice Core (TALDICE; Stenni et al., 2011). The ice core data have been processed and synchronized following the methods of Sime et al. (2009), Holloway, Sime, Singarayer, Tindall, Bunch, et al. (2016), and Holloway et al. (2017) to isolate the LIG isotope maximum, at approximately 128 ka. Our methodology results in a core-average LIG maximum $\delta^{18}O$ anomaly of +3.38‰ relative to the last 3 ka. We also compare modeled SSST (January – March [JFM]) anomalies against the Capron et al. (2014) compilation of LIG Southern Ocean SSST reconstructions. The compilation of Capron et al. (2014) uses 10-m water depth in the 1998 World Ocean Atlas as modern reference to calculate SST anomalies. We note that our simulated SSST anomalies are relative to a preindustrial experiment. However, as Southern Ocean SST trends over the twentieth century are indistinguishable from zero (McGregor et al., 2015), this is not expected to significantly affect our results. We average each synchronized SSST record over the period 128 ± 1 ka, resulting in
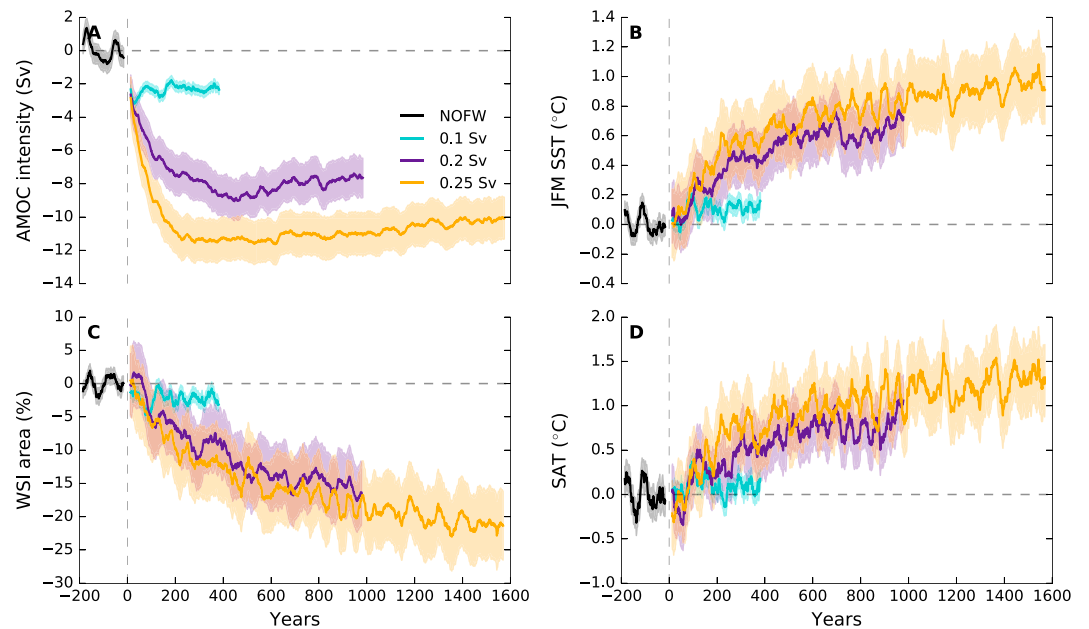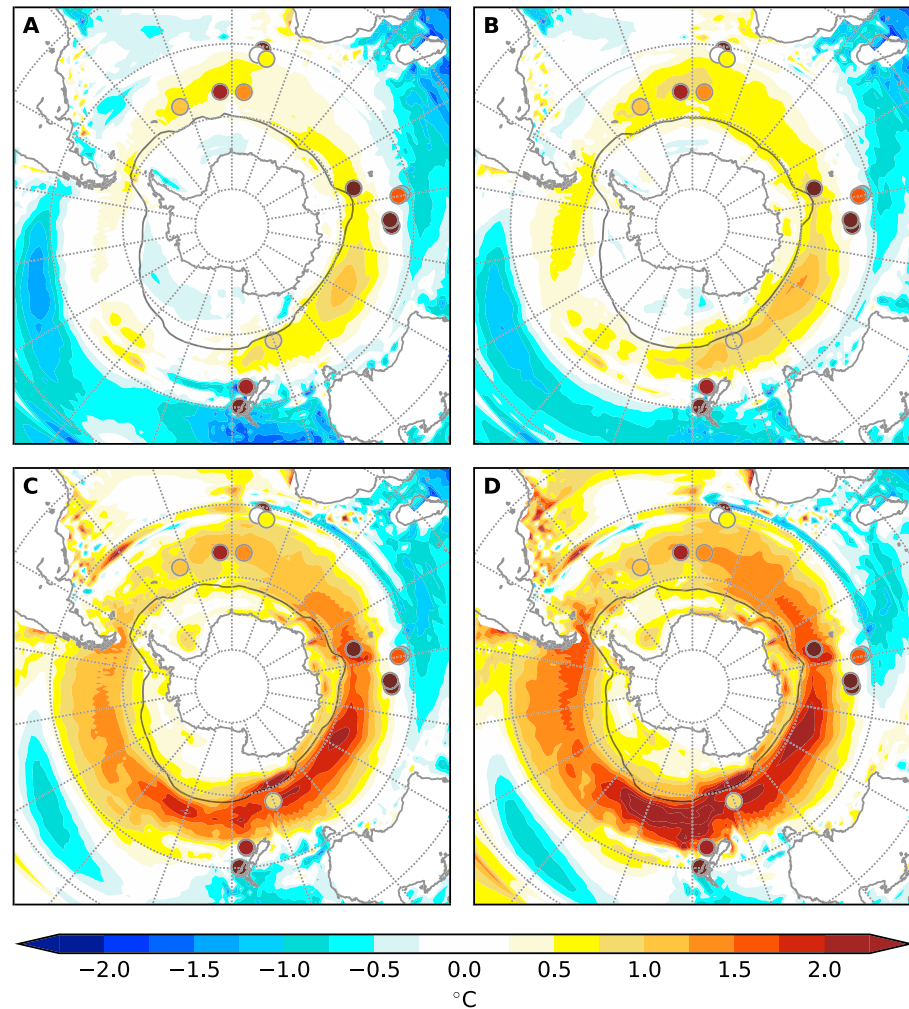
Figure 1. Climate anomalies for 128-ka experiments with no meltwater (black; NOFW), 0.1 Sv (cyan), 0.2 Sv (purple), and 0.25 Sv (orange) of meltwater added to the surface North Atlantic Ocean. Anomalies are presented relative to NOFW. Time series of (a) Atlantic Meridional Overturning Circulation (AMOC) intensity (10^6 m^3/s = 1 Sv), calculated as the maximum overturning stream function in the North Atlantic, excluding the surface wind-driven circulation; (b) Southern Ocean summer sea surface temperature (January–March [JFM]; degrees Celsius) averaged south of 50°S; (c) Southern Hemisphere winter (September) sea ice area (WSI; % change); and (d) East Antarctic annual mean surface air temperature (SAT; degrees Celsius) averaged between longitudes of 0–170°E. Bold lines show 30-year running mean, and shading indicates 1σ. Year zero signifies the start of meltwater forcing.

a marine core-average Southern Ocean SSST anomaly of +2.09 °C. For comparison, the more recent compilation of Capron et al. (2017) calculate an average Southern Ocean SSST warming of 1.8 °C for both the 127- and 130-ka time slices (standard errors of 0.8 and 0.9 °C, respectively), relative to preindustrial, whereas peak LIG temperature was reached at 129.3 ± 0.9 ka in the Southern Hemisphere and 126.4 ± 1.9 ka in the North Atlantic (Capron et al., 2014).

3. Results

Relative to the preindustrial, there is a weak climate response to 128-ka orbital and greenhouse gas forcing alone. There is negligible change in AMOC strength (−2%). There is weak warming south of 50°S in Southern Ocean SSST (+0.2 °C) and annual mean East Antarctic air temperature (+0.74 °C). Summer (JFM) East Antarctic temperature anomalies are negative (−0.63 °C). Southern Hemisphere winter maximum (September) sea ice area is reduced by 8%. Across the five East Antarctic ice core sites, the core-average annual mean surface temperature anomaly is +0.77 °C. However, the summer temperature anomaly is −0.73 °C, and the core-average δ^{18}O anomaly is −0.23‰. This does not agree with the observed Antarctic ice core isotope peak of +3.38‰ and suggests that simulations forced by radiative forcing, but no meltwater, do not have a strong impact on ice core δ^{18}O (e.g., Otto-Bliesner et al., 2013).

In each case, the addition of meltwater to the North Atlantic weakens the AMOC (Figure 1a and supporting information Figure S1), resulting in North Atlantic cooling and a southward shift of the Intertropical Convergence Zone (not shown). With 0.1 Sv of meltwater added to the North Atlantic, drifts in the AMOC stabilize within 50 years. For larger magnitudes of meltwater, the AMOC continues to weaken throughout the first 200–300 years of each experiment (Figure 1a). By the end of each integration, the AMOC has weakened by 15%, 47%, and 67% relative to PI for meltwater inputs of 0.1, 0.2, and 0.25 Sv over 400, 1,000, and 1,600 years, respectively. Since Southern Hemisphere heat transport is roughly dependent on AMOC strength, Southern Ocean and Antarctic temperatures continue to rise even after the AMOC has stabilized at a lower value (Figures 1b and 1d). After 1,600 years of 0.25-Sv meltwater input, the total ocean heat content has increased by +1.39 × 10^{22} J relative to the NOFW experiment. The largest heat gain occurs within the top 2,000 m

Figure 2. Southern Ocean summer (January–March) sea surface temperature anomalies for 128-ka experiments with (a) no meltwater; (b) 0.1 Sv over 400 years; (c) 0.2 Sv over 1,000 years; and (d) 0.25 Sv of meltwater added to the North Atlantic over 1,600 years, compared against a preindustrial control experiment. Filled circles show reconstructed sea surface temperature anomalies at 128 ka (Capron et al., 2014). Gray lines signify the 15% September sea ice concentration threshold.

($+1.26 \times 10^{22}$ J) and between latitudes of 50°S and 20°N (supporting information Figure S2). This is equivalent to ~5% of the observed increase in 0- to 2,000-m ocean heat content between 1955 and 2010 ($24 \pm 1.9 \times 10^{22}$ J; Levitus et al., 2012). In the Atlantic basin, the total heat content gain is $+0.33 \times 10^{22}$ J, largely confined to the South Atlantic (supporting information Figure S2h). Warming spreads throughout the Southern Ocean via the Antarctic Circumpolar Current (Stouffer et al., 2006), leading to Southern Ocean average SSST warming of 1.2 °C relative to PI after 1,600 years of 0.25-Sv meltwater forcing (Figure 2d). A warmer Southern Ocean leads to a retreat of Southern Hemisphere winter sea ice area of 27% relative to PI. The largest relative change in winter sea ice area occurs in the Indian sector of the Southern Ocean (−34% relative to PI), coincident with the ocean sector that features strongest warming. Warmer air temperatures extend into the continent, producing an average East Antarctic annual mean warming of 2.1 °C relative to PI (Figure 3, left panels). However, summer (JFM) temperature anomalies are far weaker; +0.75 °C or <40% of the annual mean warming. Averaging across the five ice core sites, annual mean and summer-only surface temperatures warm by 2.4 and 0.9 °C relative to PI, respectively. Annual mean warming is >2 °C at all sites but largest at EDML (+3 °C), while summer-only warming is weakest at Dome F (+0.12 °C) and largest at TALDICE and over double that at any other site (+2 °C).

The response of annual mean compared to summer-only temperatures demonstrates a change in seasonality during the LIG. This is reflected in both precipitation and temperature. Previous work has suggested
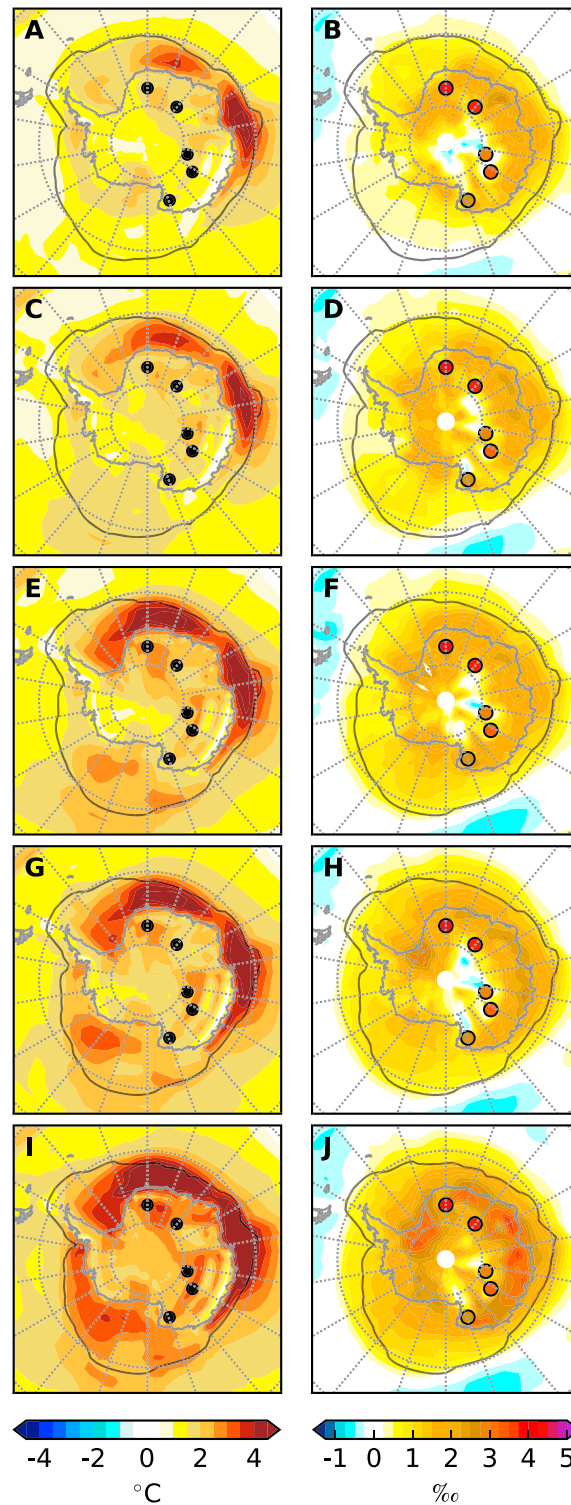
Figure 3. Anomalies in Antarctic annual mean surface air temperature (left panels: a, c, e, g, and i) and δ^{18}O (right panels: b, d, f, h, and j) for the 0.25-Sv experiment after (a, b) 200 years; (c, d) 400 years; (e, f) 600 years; (g, h) 1,000 years; and (i, j) 1,600 years of meltwater added to the North Atlantic, compared with a preindustrial control experiment. The locations and reconstructed δ^{18}O anomalies (filled circles in right panels) from the five East Antarctic ice cores are shown. Gray lines signify the 15% September sea ice concentration threshold.
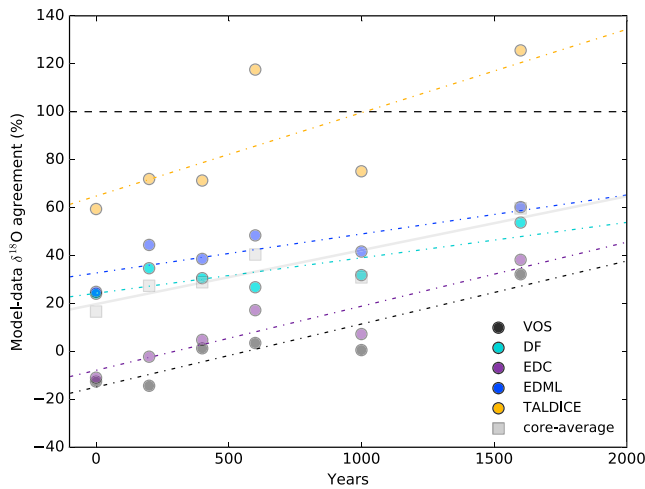
Figure 4. Model data δ^{18}O agreement (percentage of observed ice core anomaly reconstructed at 128 ka) against simulation duration for the 1,600-year 0.25-Sv experiment for each ice core site; Vostok (VOS, black circles); Dome F (DF, cyan); EPICA Dome C (EDC, purple); EPICA Dronning Maud Land (EDML, blue); Talos Dome Ice Core (TALDICE, orange); and the core average (gray squares). A linear fit is shown for the core-average as well as for each individual site, so the original phrasing is more accurate. EPICA = European Project for Ice Coring in Antarctica.

an increase in cold season (June–August [JJA]) and a decrease in warm season (December–February [DJF]) precipitation associated with warmer than present (Sime et al., 2008, 2009) and LIG (Holloway, Sime, Singarayer, Tindall, Bunch, et al., 2016) climates. We test this for our NOFW and 0.25-Sv experiments by diagnosing changes in the seasonality of precipitation at each of the ice core sites (supporting information Figure S3). We find that cold season precipitation is indeed increased, both with and without meltwater input, over most of the ice core sites. This pattern correlates with seasonal changes in Southern Ocean SST (supporting information Figure S3a); negative (positive) SST anomalies correspond to less (more) precipitation over Antarctica. Southern Ocean SST anomalies are negative during DJF (−0.5 and −0.4 °C for NOFW and 0.25 Sv, respectively) and positive during JJA (+0.6 and +0.7 °C, respectively). Seasonality changes have the strongest influence at the inland, low accumulation sites (Vostok, DF, and EDC) and is weaker at the high-accumulation, coastal sites. The change in precipitation seasonality has a negative influence on precipitation-weighted δ^{18}O falling across Antarctica. The magnitude and pattern of anomalies are similar both with and without meltwater input, suggesting that changes in precipitation seasonality are driven by the higher obliquity and lower precession during the early LIG compared to today (Yin & Berger, 2010).

Further investigation shows that this effect is not model specific. We compare the precipitation seasonality for available LIG simulations in the Paleoclimate Model Intercomparion Project (Bakker & Renssen, 2014; Lunt et al., 2013); HadCM3, CCSM3, and NorESM experiments covering 120, 125, 128, and/or 130 ka (B. Otto-Bliesner, personal communication, August, 2016). This multimodel comparison shows a robust increase in the contribution of cold season precipitation and a decrease in warm season precipitation toward the annual mean (supporting information Figure S4). The core-average, multimodel mean shows the largest decrease during DJF (−8%) and largest increase during JJA (+5%). This pattern is stronger if only the inland core sites of Vostok, DF, and EDC are considered; the DJF contribution decreases by −12% while the JJA contribution increases by +7%. In the multimodel mean, the inland core sites also show an increase in the contribution of precipitation falling between September and November (SON; +8%). This season coincides with the maximum extent of Antarctic sea ice, isolating the continent and acting to further deplete precipitation δ^{18}O at the inland core sites. The difference between the change in cold season compared to warm season precipitation (ΔJJA−ΔDJF) is −4, −2, and −1.4% for CCSM3, HadCM3, and NorESM, respectively; that is, the decrease in warm season precipitation is larger than the increase in cold season precipitation. The pattern is again larger if the coastal sites of EDML and TALDICE are removed; −5%, −3%, and −5% for CCSM3, HadCM3, and NorESM, respectively.

Although changes in seasonality have a negative influence on Antarctic δ^{18}O, the addition of meltwater and resultant warming and sea ice retreat acts to enrich δ^{18}O over the Antarctic ice core sites (Figure 3 right panels and Figure 4). Core-averaged anomalies at the end of the 1,600-year 0.25-Sv experiment are +2.02‰. This reduces the root-mean-square error from 3.6‰ for the NOFW experiment to 1.7‰ and reconciles 60% of the observed LIG Antarctic ice core isotope anomaly. Anomalies are largest at EDML and TALDICE, reaching +2.7‰ and +3.2‰, respectively. A weaker isotopic response is observed at the inland sites, Vostok, EDC, and Dome F (+0.9‰, +1.27‰, and +2.02‰, respectively). Assuming a linear relationship between the duration of meltwater input and Antarctic isotopic composition suggests that the simulated core-averaged δ^{18}O enrichment will reach 100% of the observed LIG Antarctic ice core anomaly after 3,000 years of 0.25-Sv meltwater input using the isotope-enabled HadCM3 model (Figure 4). At individual sites, the duration of meltwater input required to fully reconcile the LIG isotope peak varies from 800 years at TALDICE to 3,800 years at Vostok. The required meltwater duration at other sites converge toward ~3,500 years (3,700, 3,500, and 3,000 years for Dome F, EDC, and EDML, respectively).

4. Discussion

According to our experiments using the isotope-enabled HadCM3 model, a North Atlantic meltwater input of 0.25 Sv over 1,600 years can explain 60% of the observed isotope peak. This is consistent with the response

of other model components in the high-latitude Southern Hemisphere, including ∼55% of the LIG Southern Ocean SSST anomaly reconstructed by Capron et al. (2014) and 50% of the Southern Hemisphere winter sea ice area retreat estimated by Holloway et al. (2017).

Meltwater input to the North Atlantic not only enriches $\delta^{18}O$ at the ice core sites but also improves the spatial pattern of anomalies between sites. Intersite differences in the model-data agreement at Vostok, EDC, EDML, and Dome F reduce with increasing meltwater duration (Figure 4). A linear extrapolation implies that the model-data mismatch at these sites would be fully reconciled using simulations including 0.25-Sv meltwater forcing for 3,000–3,800 years in duration. However, this assumes continued linear trends in SSST, sea ice, and $\delta^{18}O$ and that the climate system does not reach a new equilibrium with the imposed meltwater forcing before model-data agreement is achieved. TALDICE remains an outlier, diverging from the other sites and achieving the observed ice core isotope enrichment after <1,000 years of meltwater input. This may suggest a unique ice elevation history or changes in sea ice in the TALDICE region; ice sheet thickening or less sea ice retreat in this region, as suggested by Holloway et al. (2017), might reduce the magnitude of isotopic enrichment and bring the TALDICE model-data agreement in line with other sites.

Elevation reconstructions of the East Antarctic Ice Sheet (EAIS) during the LIG are highly uncertain; evidence is unclear whether the EAIS thinned (due to increased melting) or thickened (due to an increase in accumulation), but changes were likely small on the order of a few hundred meters (Bradley et al., 2013). Thinning of the EAIS is expected to warm East Antarctica and enrich $\delta^{18}O$ (e.g., Holden et al., 2010); observational constraints suggest an average isotope-elevation relationship of +0.3‰ change in $\delta^{18}O$ per 100-m decrease in elevation in most world regions (Blisniuk & Stern, 2005; Poage & Chamberlain, 2001) but a higher value of 0.7‰ per 100 m is observed in a data set of Antarctic surface snow (Masson-Delmotte et al., 2008). Idealized elevation change experiments with HadCM3 provide a model constraint of 0.6‰ per 100 m, averaged across the East Antarctic ice core sites (work in preparation). Consequently, an elevation lowering of 200 m could generate 36–41% of the LIG $\delta^{18}O$ anomaly and, therefore, explain the remaining model-data disagreement. However, EAIS thinning would imply ice sheet melting and a synchronous freshening of the surface Southern Ocean, which would tend to cool SSTs and lead to an expansion of Southern Hemisphere sea ice (Hansen et al., 2016; Holloway, Sime, Singarayer, Tindall, Bunch, et al., 2016), worsening the model-data agreement. The 1,600-year 0.25-Sv experiment generates an effective sea level equivalent of +25 m, inferred from the change in global ocean salinity. This might suggest that a higher, and more realistic, sensitivity to meltwater forcing in HadCM3 would produce a larger climate response in these experiments and explain a greater proportion of the LIG climate anomaly.

A bipolar seesaw heat redistribution likely played an important role in the early LIG Southern Hemisphere climate optimum, at roughly 128 ka. Assuming that these model results provide a realistic simulation of Northern Hemisphere meltwater input, consistent with the likely range of HS11, and that the simulated Southern Hemisphere response is not significantly underestimated, then these results suggest that longer model integrations including meltwater forcing or a nonnegligible magnitude of EAIS surface lowering is necessary to reconcile the early LIG isotope maximum.

References

Bakker, P., & Renssen, H. (2014). Last interglacial model-data mismatch of thermal maximum temperatures partially explained. *Climate of the Past*, *10*(4), 1633–1644. https://doi.org/10.5194/cp-10-1633-2014

Blisniuk, P. M., & Stern, L. A. (2005). Stable isotope paleoaltimetry: A critical review. *American Journal of Science*, *305*(10), 1033–1074. https://doi.org/10.2475/ajs.305.10.1033

Bond, G. C., & Lotti, R. (1995). Iceberg discharges into the North Atlantic on millennial time scales during the last glaciation. *Science*, *267*, 1005–1010. https://doi.org/10.1126/science.267.5200.1005

Bradley, S. L., Siddall, M., Milne, G. A., Masson-delmotte, V., & Wolff, E. (2013). Combining ice core records and ice sheet models to explore the evolution of the east Antarctic ice sheet during the last interglacial period. *Global and Planetary Change*, *100*, 278–290. https://doi.org/10.1016/j.gloplacha.2012.11.002

Broecker, W. S., & Henderson, G. M. (1998). The sequence of events surrounding termination II and their implications for the cause of glacial-interglacial CO_2 changes. *Paleoceanography*, *13*(4), 352–364.

Capron, E., Govin, A., Feng, R., Otto-Bliesner, B. L., & Wolff, E. W. (2017). Critical evaluation of climate syntheses to benchmark CMIP6/PMIP4 127 ka last interglacial simulations in the high-latitude regions. *Quaternary Science Reviews*, *168*, 137–150. https://doi.org/10.1016/j.quascirev.2017.04.019

Capron, E., Govin, A., Stone, E. J., Masson-Delmotte, V., Mulitza, S., Otto-Bliesner, B. L., et al. (2014). Temporal and spatial structure of multi-millennial temperature changes at high latitudes during the last interglacial. *Quaternary Science Reviews*, *103*, 116–133. https://doi.org/10.1016/j.quascirev.2014.08.018

Clark, P. U., Pisias, N. G., Stocker, T. F., & Weaver, A. J. (2002). The role of the thermohaline circulation in abrupt climate change. *Science*, *415*, 863–869. https://doi.org/10.1126/science.1081056

Duplessy, J. C., Labeyrie, L., Arnold, M., Paterne, M., Duprat, J., & van Weering, T. C. E. (1992). Changes in surface salinity of the north atlantic ocean during the last deglaciation. *Nature*, *358*, 485–488.

EPICA Community Members (2006). One-to-one coupling of glacial climate variability in Greenland and antarctica. *Nature*, *444*(7116), 195–198. https://doi.org/10.1038/nature05301

Ferguson, G., & Jasechko, S. (2015). The isotopic composition of the Laurentide ice sheet and fossil groundwater. *Geophysical Research Letters*, *42*, 4856–4861. https://doi.org/10.1002/2015GL064106

Govin, A., Braconnot, P., Capron, E., Cortijo, E., Duplessy, J.-C., Jansen, E., et al. (2012). Persistent influence of ice sheet melting on high northern latitude climate during the early last interglacial. *Climate of the Past*, *8*(2), 483–507. https://doi.org/10.5194/cp-8-483-2012

Govin, A., Capron, E., Tzedakis, P. C., Verheyden, S., Ghaleb, B., Hillaire-Marcel, C., et al. (2015). Sequence of events from the onset to the demise of the last interglacial: Evaluating strengths and limitations of chronologies used in climatic archives. *Quaternary Science Reviews*, *129*, 1–36. https://doi.org/10.1016/j.quascirev.2015.09.018

Hansen, J., Sato, M., Hearty, P., Ruedy, R., Kelley, M., Masson-Delmotte, V., et al. (2016). Ice melt, sea level rise and superstorms: Evidence from paleoclimate data, climate modeling, and modern observations that 2°C global warming could be dangerous. *Atmospheric Chemistry and Physics*, *16*(6), 3761–3812. https://doi.org/10.5194/acp-16-3761-2016

Hill, H. W., Flower, B. P., Quinn, T. M., Hollander, D. J., & Guilderson, T. P. (2006). Laurentide ice sheet meltwater and abrupt climate change during the last glaciation. *Paleoceanography*, *21*, PA1006. https://doi.org/10.1029/2005PA001186

Hoffman, J. S., Clark, P. U., Parnell, A. C., Andrew, C., & Feng, H. (2017). Regional and global sea-surface temperatures during the last interglaciation. *Science*, *355*, 276–279. https://doi.org/10.1126/science.aai8464

Holden, P. B., Edwards, N. R., Wolff, E. W., Lang, N. J., Singarayer, J. S., Valdes, P. J., & Stocker, T. F. (2010). Interhemispheric coupling, the west Antarctic ice sheet and warm Antarctic interglacials. *Climate of the Past*, *6*(4), 431–443. https://doi.org/10.5194/cp-6-431-2010

Holloway, M. D., Sime, L. C., Allen, C. S., Hillenbrand, C. D., Bunch, P., Wolff, E., & Valdes, P. J. (2017). The spatial structure of the 128 ka Antarctic sea ice minimum. *Geophysical Research Letters*, *44*, 11,129–11,139. https://doi.org/10.1002/2017GL074594

Holloway, M. D., Sime, L. C., Singarayer, J. S., Tindall, J. C., Bunch, P., & Valdes, P. J. (2016). Antarctic last interglacial isotope peak in response to sea ice retreat not ice-sheet collapse. *Nature Communications*, *7*(12), 293.

Holloway, M. D., Sime, L. C., Singarayer, J. S., Tindall, J. C., & Valdes, P. J. (2016). Reconstructing paleosalinity from δ18O: Coupled model simulations of the last glacial maximum, last interglacial and late Holocene. *Quaternary Science Reviews*, *131*, 350–364. https://doi.org/10.1016/j.quascirev.2015.07.007

Jouzel, J., Masson-Delmotte, V., Cattani, O., Dreyfus, G., Falourd, S., Hoffmann, G., et al. (2007). Orbital and millennial antarctic climate variability over the past 800,000 years. *Science*, *317*(5839), 793–796. https://doi.org/10.1126/science.1141038

Kawamura, K., Parrenin, F., Lisiecki, L., Uemura, R., Vimeux, F., Severinghaus, J. P., et al. (2007). Northern Hemisphere forcing of climatic cycles in Antarctica over the past 360,000 years. *Nature*, *448*(7156), 912–916. https://doi.org/10.1038/nature06015

Levitus, S., Antonov, J. I., Boyer, T. P., Baranova, O. K., Garcia, H. E., Locarnini, R. A., et al. (2012). World ocean heat content and thermosteric sea level change (0-2000m), 1955-2010. *Geophysical Research Letters*, *39*, L10603. https://doi.org/10.1029/2012GL051106

Lunt, D. J., Abe-Ouchi, A., Bakker, P., Berger, A., Braconnot, P., Charbit, S., et al. (2013). A multi-model assessment of last interglacial temperatures. *Climate of the Past*, *9*(2), 699–717. https://doi.org/10.5194/cp-9-699-2013

Marino, G., Rohling, E. J., Rodríguez-Sanz, L., Grant, K. M., Heslop, D., Roberts, A. P., et al. (2015). Bipolar seesaw control on last interglacial sea level. *Nature*, *522*(7555), 197–201. https://doi.org/10.1038/nature14499

Masson-Delmotte, V., Buiron, D., Ekaykin, A., Frezzoti, M., Gallée, H., Jouzel, J., et al. (2011). A comparison of the present and last interglacial periods in six Antarctic ice cores. *Climate of the Past*, *7*(2), 397–423. https://doi.org/10.5194/cp-7-397-2011

Masson-Delmotte, V., Jouzel, J., Cattani, O., Delmotte, M., Falourd, S., Landais, A., et al. (2008). A review of Antarctic surface snow isotopic composition: Observations, atmospheric circulation, and isotopic modeling. *Journal of Climate*, *21*, 3359–3387. https://doi.org/10.1175/2007JCLI2139.1

McGregor, H. V., Evans, M. N., Goosse, H., Leduc, G., Martrat, B., Addison, J. A., et al. (2015). Robust global ocean cooling trend for the pre-industrial common era. *Nature Geoscience*, *8*(9), 671–677. https://doi.org/10.1038/ngeo2510

Otto-Bliesner, B. L., Rosenbloom, N., Stone, E. J., McKay, N. P., Lunt, D. J., Brady, E. C., & Overpeck, J. T. (2013). How warm was the last interglacial? New model-data comparisons. *Philisophical Transactions of the Royal Society A*, *371*(20130097). https://doi.org/10.1098/rsta.2013.0097

Peltier, W. R. (2004). Global glacial isostasy and the suraface of the ice-age Earth: The ICE-5g (VM2) model and GRACE. *Annual Review of Earth and Planetary Sciences*, *32*, 111–149. https://doi.org/10.1146/annurev.earth.32.082503.144359

Peltier, W. R., & Vettoretti, G. (2014). Dansgaard-Oeschger oscillations predicted in a comprehensive model of glacial climate: A "kicked" salt oscillator in the Atlantic. *Geophysical Research Letters*, *41*, 7306–7313. https://doi.org/10.1002/2014GL061413

Petit, J. R., Jouzel, J., Raynaud, D., Barkov, N. I., Barnola, J.-M., Basile, I., et al. (1999). Climate and atmospheric history of the past 420,000 years from the Vostok ice core, Antarctica. *Nature*, *399*, 429–436.

Poage, M. A., & Chamberlain, C. P. (2001). Empirical relationships between elevation and the stable isotope composition of precipitation and surface waters: Considerations for studies of paleoelevation change. *American Journal of Science*, *301*(1), 1–15. https://doi.org/10.2475/ajs.301.1.1

Sime, L. C., Tindall, J. C., Wolff, E. W., Connolley, W. M., & Valdes, P. J. (2008). Antarctic isotopic thermometer during a CO_2 forced warming event. *Journal of Geophysical Research*, *113*, D24119. https://doi.org/10.1029/2008JD010395

Sime, L. C., Wolff, E. W., Oliver, K. I. C., & Tindall, J. C. (2009). Evidence for warmer interglacials in east Antarctic ice cores. *Nature*, *462*, 342–345. https://doi.org/10.1038/nature08564

Stenni, B., Buiron, D., Frezzotti, M., Albani, S., Barbante, C., Bard, E., et al. (2011). Expression of the bipolar see-saw in Antarctic climate records during the last deglaciation. *Nature Geoscience*, *4*(1), 46–49. https://doi.org/10.1038/ngeo1026

Stocker, T. F., & Johnsen, S. J. (2003). A minimum thermodynamic model for the bipolar seesaw. *Paleoceanography*, *18*(4), 1087. https://doi.org/10.1029/2003PA000920

Stone, E. J., Capron, E., Lunt, D. J., Payne, A. J., Singarayer, J. S., Valdes, P. J., & Wolff, E. W. (2016). Impact of melt water on high latitude early last interglacial climate. *Climate Past Discuss*, *12*(9), 1–22. https://doi.org/10.5194/cp-2016-11

Stouffer, R. J., Yin, J., Gregory, J. M., Kamenkovich, I. V., & Sokolov, A. (2006). Investigating the causes of the response of the thermohaline circulation to past and future climate changes. *Journal of Climate*, *19*(8), 1365–1387. https://doi.org/10.1175/JCLI3689.1

Tindall, J. C., Valdes, P. J., & Sime, L. C. (2009). Stable water isotopes in HadCM3: Isotopic signature of El Niño—Southern Oscillation and the tropical amount effect. *Journal of Geophysical Research*, *114*, D04111. https://doi.org/10.1029/2008JD010825

WAIS Divide Project Members (2013). Onset of deglacial warming in west antarctica driven by local orbital forcing. *Nature*, *500*(7463), 440–4. https://doi.org/10.1038/nature12376

WAIS Divide Project Members (2015). Precise interpolar phasing of abrupt climate change during the last ice age. *Nature*, *520*, 661–665. https://doi.org/10.1038/nature14401

Yin, Q. Z., & Berger, A. (2010). Insolation and CO_2 contribution to the interglacial climate before and after the mid-Brunhes event. *Nature Geoscience*, *3*(4), 243–246. https://doi.org/10.1038/ngeo771